

SPARS: THE SYSTEM, ALGORITHMS, AND TEST RESULTS¹

N. F. Toda, J. L. Heiss, and F. H. Schlee
IBM Federal Systems Division
Owego, New York

ABSTRACT

SPARS - A Space Precision Attitude Reference System has three major subsystems: an Inertial Reference Unit, a Star Sensor Assembly, and a Digital Computer Subsystem. The IRU consists of three strapdown gyros employing pulse torque servo amplifiers for rebalancing. The star sensor assembly is a two-axis pitch within roll gimbaled telescope. The computer subsystem issues pointing commands to the telescope and processes measurement data from the star sensor assembly and the inertial reference unit to obtain an "optimal" estimate of spacecraft attitude. This paper describes the IBM system configuration and the performance achieved during laboratory testing.

I. INTRODUCTION

SPARS, a Space Precision Attitude Reference System, consists of: an Inertial Reference Unit, a Star Sensor Assembly, and a Digital Computer Subsystem. The Inertial Reference Unit (IRU) effectively serves as the attitude memory between star sightings. It consists of three strapdown gyros employing pulse torque servo amplifiers for re-balancing. The Star Sensor Assembly (SSA) is a two-axis, pitch within roll gimbaled telescope. Digital readout is provided by incremental gimbal encoders and silicon digital detectors. The latter measures the position of the star image within the field of view of the telescope. The computer subsystem issues pointing commands to the telescope and processes measurement data from the SSA and IRU to obtain an "optimal" estimate of spacecraft attitude.

To demonstrate the accuracy of SPARS for a spacecraft that is controlled to be nominally aligned to the local vertical, an extensive laboratory development program was undertaken to provide a very accurate test bed for the SPARS equipment. The principal laboratory subsystems were a precision rate table and star simulators. The IRU and the SSA were mounted on the rate table which provided both a velocity environment and an independent measurement of attitude.

Quaternions or Euler four parameters were employed to represent attitude rather than direction cosines or Euler angles. The attitude integration algorithm is particularly simple in this representation. The Kalman filter was employed to process the star sensor data into "optimal" estimates of spacecraft attitude.

This paper describes the IBM SPARS configuration and the performance achieved during laboratory testing. Some qualitative data are included in the main text; quantitative test results and conclusions appear in the classified (SECRET) appendix to this paper. Laboratory test equipment and procedures are discussed by Schlee and Nielsen in Reference (1). A description of the IRU used is given by Baum and Sheldon in Reference (2).

II. SPARS CONFIGURATION

The IBM SPARS configuration consists of: a strapdown Inertial Reference Unit (IRU), a gimbaled Star Sensor Assembly (SSA), and an onboard computer which utilizes a software package employing Kalman filtering techniques.

The IRU is ideally suited for orbital applications where relatively low angular rates are experienced. The gimbaled star sensor supplements the inertial

¹Work described in this paper was performed under Contract F04701-63-C-0225.

packages by providing regular and frequent attitude updates via celestial "fixes." High resolution of the star position is realized by utilizing a gimballed telescope with a small Field of View (FOV).

The IRU consists of three integrating gyroscopes operated in a forced limit cycle rebalance loop. The output of the gyroscopes is in the form of pulse counts which are proportional to the integral of the body angular rates.

The SSA features gray-coded silicon coordinate readout devices combined with a pitch within roll gimbal design. The purpose of the silicon coordinate readout device, which is subsequently referred to as a digital readout, is to measure the X and Y coordinates of the star image within the telescope FOV. This provides a measurement of the star line of sight relative to the telescope axis; orientation of the telescope relative to the SPARS base plate is provided by the pitch and roll gimbal encoders. The X and Y coordinate measurements and the pitch and roll gimbal angle measurements were combined by the SPARS software into pitch and roll angles which defined the star line of sight orientation relative to the SPARS base plate. It is these angles which were input to the Kalman filter.

The SSA was designed to operate in a non-nulling mode, i.e., the gimbal drive servos were not driven so that the star image lies in the center of the telescope FOV. Instead, the telescope was driven so that the star image remains within the FOV and has no relative motion. Motion of the star image across the digital detector would smear the star image and would result in X and Y coordinate readout errors.

The non-nulling approach was selected to permit use of a rate servo rather than a position servo, thereby minimizing the gimbal servo design and improving star image detection. Since the star image remains motionless on the sensitive digital detector grid, the image signal-to-noise ratio can be increased by lengthening the image exposure time.

The SSA developed, fabricated, and demonstrated during the SPARS Phase 1A effort is physically made up of two components: the gimballed telescope and the electronics cabinet. Figure 1 shows the SSA. The functional breakdown of these two components is illustrated in Figure 2.

III. DIGITAL DETECTOR AND TELESCOPE

The digital detectors are silicon photovoltaic sensors employing a gray coded binary pattern which produces a direct digital readout of a line image that impinges on the pattern. The line image is generated by the optics which include cylindrical elements. Pre-amplification electronics for digital detector outputs are contained in the telescope assembly. Be-

cause the detailed description of the optical prescription, the digital detectors, and their associated signal processing circuits are of a proprietary nature, they are not included in this paper. The overall telescope FOV, which is defined by the optical prescription and the digital detector cell dimension, is 600 arc seconds. An additional element exists between the cylindrical lens and the detector cell to provide star signal modulation.

The overall gimbal assembly employs a cantilever design rather than the conventional gimbal design. Figure 1 shows the case of the roll gimbal serving as the mounting fixture to the spacecraft. The pitch gimbal assembly is mounted on the roll gimbal shaft and the telescope assembly is mounted on the pitch gimbal shaft. Gimbals were free to rotate through at least 90 degrees.

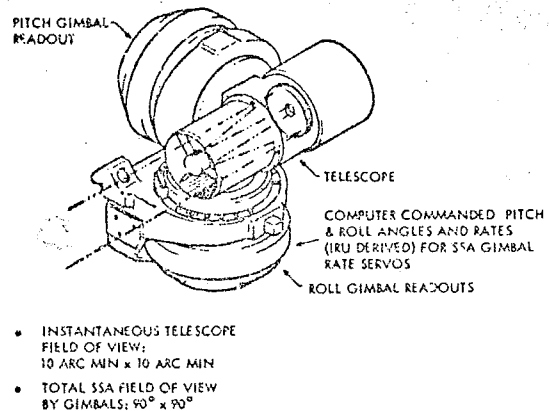


Fig.1. SSA

Beginning with warmup and star sensor energization and self-test, an operational sequence consisting of star search and acquisition is performed. SPARS is designed to determine precisely the attitude of a vehicle whose attitude is already known to an accuracy of $\pm 2\text{-}1/4$ degrees per axis. Thus the initial star acquisition problem for the SPARS consists of searching for a star within a cone having a half angle of $2\text{-}1/4$ degrees. Because the probability of the first three stars falling within the 10×10 arc minute field-of-view of the star sensor is very low, a search mode is implemented for acquisition. Following the first three star fixes, knowledge of the attitude is improved to the point that subsequent star sensor pointing commands will assure that the star falls within the telescope FOV. Subsequent star fixes at 30 second intervals then are processed with the on-board filter to improve the attitude estimate, to calibrate the IRU gyros, and to estimate star sensor misalignments. Operational utilization of SPARS requires only a single instantaneous snapshot of a star once every 30

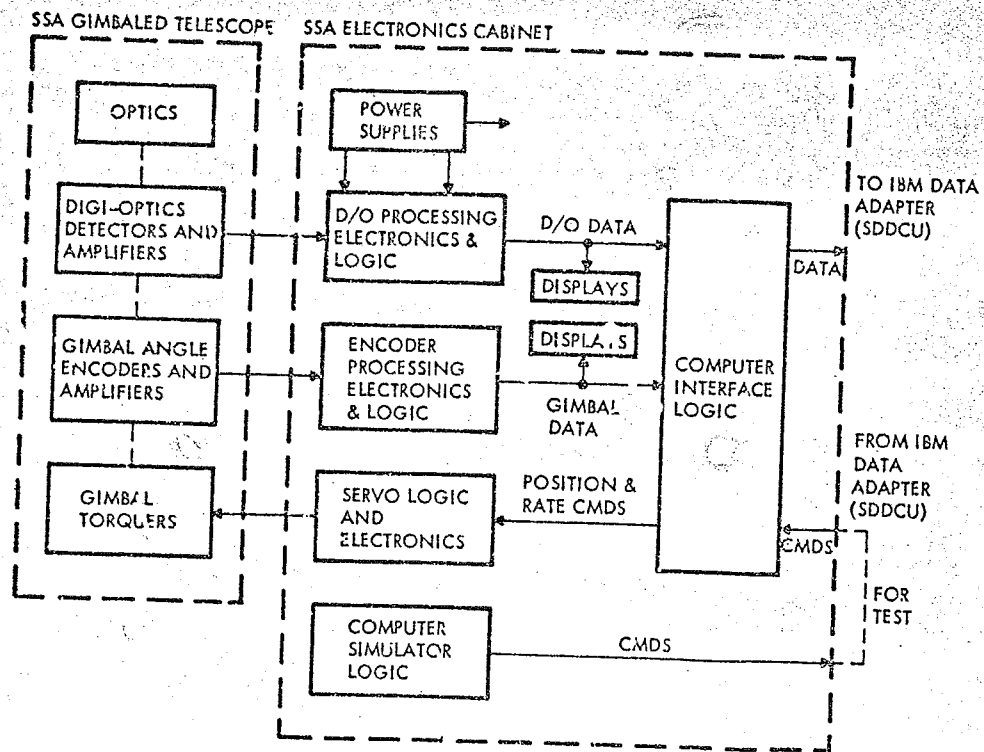


Fig. 2. SSA Functional Diagram

seconds. The attitude during the interval between these fixes is remembered by the IRU gyros, which will have been calibrated by the SPARS software. The IRU data is sampled every 125 milliseconds to provide a relatively continuous estimate of spacecraft attitude.

IV. SPARS LABORATORY OPERATING CONCEPT

The Phase IA laboratory implementation of the SPARS hardware and software required some modifications from the orbital case in order to accommodate the earthbound laboratory environment (e.g., the influence of earth's rate on the IRU gyros) and the absence of the search function in the SSA feasibility model. The laboratory operation therefore was constrained to initial attitude errors of less than ± 5 arc minutes as dictated by the SSA telescope FOV. The arrangement of the star simulator in the IBM SPARS Laboratory was such that only one quarter of an orbit could be traversed with a regularity of star sightings. However, this approximately 20 minute test duration was sufficient to demonstrate optimal filter convergence and steady-state behavior. Full orbit operation in the laboratory also was performed with attitude maintenance during the additional

3/4 orbit travel wholly dependent on the calibrated gyro performance.

V. ATTITUDE REPRESENTATION

There are many sets of dependent variables which can be employed to represent the attitude of the spacecraft. The most common are Euler angles, the direction cosine matrix, and quaternions*. The kinematic equations describing the attitude may be written as

$$\frac{dp}{dt} = f(p, w)$$

where p denotes the variables which represent spacecraft attitude and w denotes the vehicle angular velocity. Euler angles have the advantage that only three parameters are required, and the disadvantage that the vector function $f(p, w)$ is a transcendental function of p . The direction cosine matrix and quaternion representation require nine and four parameters respectively, but have the advantage that f is a linear function of p .

SPARS employs quaternions to represent the orientation of the body relative to an inertial frame.

*Quaternions are sometimes called Euler four parameter or Cayley-Klein parameters. The four parameter representation was first derived by Euler before Hamilton developed quaternions.

The reasons for employing quaternions (see References 3 and 4) are:

- $f(p, w)$ is linear in p
- quaternions utilize only four parameters to specify attitude in contrast to nine when direction cosines are used
- the time history of spacecraft attitude is given by the integration of a vector differential equation instead of a matrix differential equation resulting in fewer computations per integration step
- "renormalization" of the quaternions is much more simply accomplished than the corresponding operation for direction cosines. The significance of the renormalization operation will be explained subsequently when the numerical integration of the attitude differential equation is discussed.

An aid to understanding quaternions can be derived from Euler's theorem which states that any sequence of rotations utilized to bring two orthogonal reference frames into coincidence is equivalent to a single rotation about some fixed axis. Let $\mu(t)$ be the angle of rotation and let $\alpha(t)$, $\beta(t)$ and $\gamma(t)$ be the direction cosines defining the fixed axis.

The quaternion elements $q_i(t)$, $i = 1, 2, 3, 4$ are

$$\begin{aligned} q_1(t) &= \cos \alpha(t) \sin (\mu(t)/2) \\ q_2(t) &= \cos \beta(t) \sin (\mu(t)/2) \\ q_3(t) &= \cos \gamma(t) \sin (\mu(t)/2) \\ q_4(t) &= \cos (\mu(t)/2) \end{aligned}$$

The quaternion representation of the kinematic equations becomes

$$\frac{dq}{dt} = \frac{1}{2} \Omega q \quad (2)$$

where Ω is the skew symmetric matrix

$$\Omega = \begin{bmatrix} 0 & w_3 & -w_2 & w_1 \\ -w_3 & 0 & w_1 & w_2 \\ w_2 & -w_1 & 0 & w_3 \\ -w_1 & -w_2 & -w_3 & 0 \end{bmatrix} \quad (3)$$

and w_i denotes the spacecraft angular velocity in body coordinates.

The solution of (2) is approximately

$$q(t) = \exp \left[G(t) \right] q(t_k) \quad (3)$$

where

$$G(t) = \Omega(t_k)(t-t_k) \quad (4)$$

This formulation was an appropriate one to be employed in SPARS since angular increments rather than rates are the outputs of the gyros. The elements of $G(t)$ are $w_i(t-t_k)$, which is the angular change about the i th body axis during the time interval (t_k, t) assuming that rates are constant during this interval. For the SPARS application, rates are almost constant except during short attitude control thrusting intervals.

A hierarchy of integration algorithms can be developed by replacing the exponential by its power-series expansion. Such a hierarchy has been constructed by Wilcox (4). In the SPARS application, algorithms of higher than second order generally did not exhibit the accuracy predicted by theoretical analysis. This is because the gyro outputs are quantized and therefore available only to limited accuracy. The accuracy of the second order algorithm can be improved by replacing it by a "modified second order" algorithm as suggested by Wilcox (loc cit). This modified second order algorithm can be expressed by the equation:

$$q(t) = \left[I \left(1 - \frac{c(t)}{12} \right) + \frac{G(t)}{2} \right] q(t_k) \quad (5)$$

where

$$c(t) = \sum_{i=1}^3 \left[\int_{t_k}^t w_i(\tau) d\tau \right]^2$$

and I is the identity matrix. In the development of (5), use has been made of the relation:

$$G(t)^2 = -c(t)I$$

The quaternion produced by the integration algorithm (5) will gradually depart from normality in the sense that the scalar

$$\sum_{i=1}^4 q_i^2(t) \quad (6)$$

will differ from unity as the integration proceeds. This effect can be compensated by periodic renormalization, i. e., by dividing the elements of the quaternion produced by (5) by the scalar (6). By utilizing the properties of quaternion norms it is easy to show that no accuracy is lost by normalization at every N th step rather than at every step. Therefore the normalization need be undertaken only when attitude information is needed for calculation external to the attitude integration.

The simplicity of the normalization correction for quaternion integration is quite in contrast to the corresponding procedure for direction cosines. Integration of the differential equations for the direction cosine representation of attitude requires not only a periodic renormalization of the rows (or columns) of the direction cosine matrix, but a re-orthogonalization of the rows (or columns).

VI. FILTER FORMULATION

The actual orientation of the SPARS attitude reference frame differed from the estimate of its orientation produced by the computer because of errors in the initial estimate of attitude and because of drifts in the gyros. The objective of the Kalman filter was to estimate, by a sequence of sightings on selected stars, the attitude error and the bias components of the gyro drift rates producing these errors. Estimation began with initialization of the filter to the current best estimate of the body attitude reference frame and gyro drift biases. This estimate of attitude was propagated to the time of the first star sighting by the integration of the quaternion. At the time of the first star sighting, the estimates of the pitch and roll angles of the line of sight to the star (computed on the basis of the computer's estimate of attitude) were compared with the measured pitch and roll angles. The differences were multiplied by the Kalman filter weighting matrix to produce corrections to the estimates of attitude and gyro drift biases. Utilizing the new estimates of attitude, the attitude quaternion was re-initialized, the gyro outputs were compensated by the new estimates of gyro biases, and the attitude differential equations integrated to the time of the next star sighting where the update procedure followed at the first star sighting was repeated. This procedure continued as long as star sightings were taken.

The usual formulation of a linear filter problem requires a linearization of (2) about the best current estimate of the state. Straightforward application of this technique would result in at least seven state variables: four representing deviations in the elements of the quaternion and three for the gyro drift biases. The filter so designed would have to incorporate a constraint on state variables since the quaternion must have unit norm.

To reduce the dimension of the state vector to six elements and to remove the constraint on the state vector, the very small attitude error was represented by three (infinitesimal) angular rotations ψ_i , $i = 1, 2, 3$ about the three body axes.

Let $\hat{w}_C = (\hat{w}_1, \hat{w}_2, \hat{w}_3)^T$ and $w_C = (w_1, w_2, w_3)^T$ denote the angular velocities of the computed and true body frames respectively. The circled subscript denotes the frame in which the components are evaluated. The angular velocity of the computed frame in

components along the true axes is

$$\hat{w}_C = \hat{w}_T + \dot{\psi} \begin{bmatrix} 1 & -\psi_3 & \psi_2 \\ \psi_3 & 1 & -\psi_1 \\ -\psi_2 & \psi_1 & 1 \end{bmatrix} \begin{bmatrix} \hat{w}_1 \\ \hat{w}_2 \\ \hat{w}_3 \end{bmatrix} \quad (6)$$

Rearrange terms to obtain

$$\begin{bmatrix} \dot{\psi}_1 \\ \dot{\psi}_2 \\ \dot{\psi}_3 \end{bmatrix} \begin{bmatrix} 0 & \hat{w}_3 & -\hat{w}_2 \\ -\hat{w}_3 & 0 & \hat{w}_1 \\ \hat{w}_2 & -\hat{w}_1 & 0 \end{bmatrix} \begin{bmatrix} \psi_1 \\ \psi_2 \\ \psi_3 \end{bmatrix} = \begin{bmatrix} \hat{w}_1 - w_1 \\ \hat{w}_2 - w_2 \\ \hat{w}_3 - w_3 \end{bmatrix}$$

Although the gyros are physically mounted along the true body axes, they sense a combination of true rate w plus drift b and noise η ; the computer assigns the sensor outputs in the computed body frame; i. e.,

$$\hat{w}_C = w_C + b_C + \eta_C$$

Assuming gyro drift is constant and their input axes are perfectly aligned with the true body axes we obtain the system equation

$$\frac{d}{dt} \begin{bmatrix} \psi \\ \delta b \end{bmatrix} = \begin{bmatrix} \Omega^* & I \\ 0 & 0 \end{bmatrix} \begin{bmatrix} \psi \\ \delta b \end{bmatrix} + \begin{bmatrix} \eta \\ 0 \end{bmatrix} \quad (7)$$

where Ω^* denotes the upper (3×3) submatrix of Ω and η denotes gyro or process noise. Additional state variables could be added to include other dynamical biases and instrument biases. (See Section 7.)

The measurements are the roll ϕ and pitch θ angles of the line of sight to a star. These pseudo-measurements are the roll and pitch obtained by combining gimbal angle encoder and digital detector readings into equivalent roll and pitch angles of the LOS. The observation errors are related to the state variables by

$$\begin{bmatrix} \delta \phi \\ \delta \theta \end{bmatrix} = \begin{bmatrix} H_1 & O \\ H_2 & O \end{bmatrix} \begin{bmatrix} \psi \\ \delta b \end{bmatrix} + \nu = H \begin{bmatrix} \psi \\ \delta b \end{bmatrix} + \nu \quad (8)$$

where ν represents the SSA instrument noise. Under suitable conditions on the statistics of the state variables at the initial time, the process noise η and the instrument noise ν we have formulated a canonical linear filter problem in equations (7) and (8). In this formulation, the gyro readings are not considered to be measurements in the usual filter sense since they do not appear in (8). If the dynamical equations of motion describing spacecraft attitude were employed to predict attitude, then gyroscope outputs could be employed as additional "filter" measurements.

VII. FILTER IMPLEMENTATION

The organization of the SPARS on-board software,

including the attitude filter, is shown in Figure 3. The filter gain matrix computations were based on:

$$W_i = P_i(-) H_i^T [H_i P_i(-) H_i^T + R]^{-1}$$

$$P_i(+) = (I - W_i H_i) P_i(-) (I - W_i H_i)^T + W_i R W_i^T$$

$$P_{i+1}(-) = \Phi(t_{i+1}, t_i) P_i(+) \Phi^T(t_{i+1}, t_i) + Q_i$$

$P(-)$ is the covariance of the state vector immediately before the i th observation, $P_i(+)$ is the covariance immediately after the i th observation. H_i is the gradient of the i th pitch and roll observation relative to the filter states, R is the covariance of the measurement noise, Q_i is the covariance of the noise accumulated in the interval (t_i, t_{i+1}) due to random gyro noise. Finally, $\Phi(t_i, t_{i+1})$ is the transition matrix for the state vector.

The Kalman filter estimates a differential correction to the state, i. e., :

$$\begin{bmatrix} \psi(t_i) \\ \delta b(t_i) \end{bmatrix} = W \begin{bmatrix} \tilde{\phi}_i - \hat{\phi}_i \\ \tilde{\theta}_i - \hat{\theta}_i \end{bmatrix}$$

where the tilde denotes measured values and the hat denotes estimates. The estimate $\psi(t_i)$ is transformed into an update of the quaternion by the formula

$$q(t_i^+) = q(t_i^-) - \frac{1}{2} S(t_i) q(t_i^-)$$

where $S(t)$ is a skew symmetric matrix having same form as Ω with w_j replaced by $\psi_j(t_i)$. It is easily

shown that if $q(t^-)$ has a unit norm then $q(t^+)$ also has unit norm. The gyro drift bias is updated by

$$b(b_i^+) = b(b_i^-) + \delta b(t_i).$$

The formula selected for the update of the filter covariance at star observation time differs from the customary formula which is

$$P(t_i^+) = P(t_i^-) - W_i H_i P(t_i^-) = (I - W_i H_i) P(t_i^-)$$

The selected formulation which can be found in many references, e.g., in the text by Bryson and Ho (3) was chosen for implementation in the filter since it is less sensitive to roundoff errors.

VIII. ERROR MODEL

Errors in the measurements were characterized either as a zero mean independent random sequence or a zero mean random variable. The random sequences combine to form the measurement and process noise errors which were represented in the filter equations by the covariance matrices R and Q respectively. Biases were modeled as random variables. Certain bias errors can be included in the filter state. This is discussed further in Section VI of Reference (1).

Bias errors were associated with alignment calibration. SSA alignment errors occurred in the measured (calibrated) alignment of: (1) the pitch and roll gimbal axes ($\gamma_{RX}, \gamma_{RZ}, \gamma_{PX}, \gamma_{PY}$) and (2) telescope (optic) axis with respect to the gimbal axes (γ_{OY}, γ_{OZ}); γ denotes the angular orientation. The first subscript refers to either the roll, pitch or optic axis and the second subscript the axis of rotation.

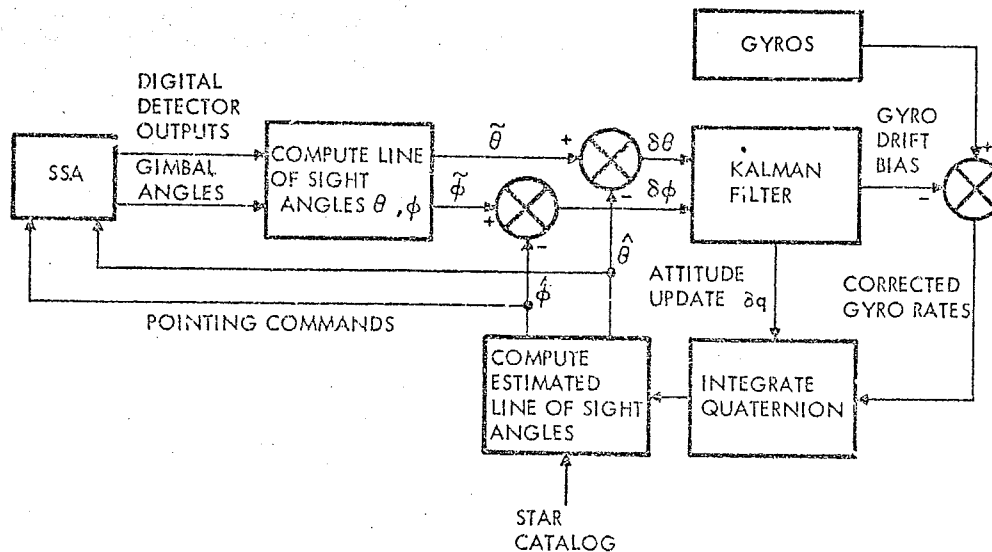


Fig. 3. On-Board Software

The errors consist of: (1) bias error in the instrument alignment and calibration; (2) cyclic error in the modeling of repeatable bearing motion; (3) random error in the form of non-repeatable bearing motion; and (4) thermal and gravity induced bending. SSA thermal bending errors were negligibly small in the controlled laboratory environment. Gravity induced bending in the laboratory was assumed to be negligible except for the roll gimbal. However, test results indicate that this may have been a poor assumption (Reference 1). The X, Y, and Z gyro input axes were not perfectly aligned with the coordinates defined by the IRU optical cube. However, uncertainty in these alignments had negligible effect on SPARS performance.

The noise-like random sequence errors are associated with read-out and fabrication errors. The readout errors include resolution (quantization) and fabrication of the readout devices, the gimbal encoders and the digital detectors. Resolution limitations impose uniformly distributed errors with maxima equal to one-half the magnitude of the least significant bit readout. Fabrication errors arise from imprecision in manufacture and the resultant inaccuracies of extrapolation techniques. Fabrication errors are for the most part repeatable at each readout position. However, the likelihood of a particular readout position recurring with significant frequency during a test run was sufficiently small to allow modeling of fabrication error as a random phenomenon.

The digital detector error model includes: resolution (quantization) and fabrication, servo-induced image motion, and thermal and gravity induced bending of the telescope. Over the long term, the detector quantization error appears to be uniformly distributed with standard deviation of $QD/\sqrt{12}$, where QD is the resolution of the detector, while the normal error due to fabrication has magnitude of σ_{FO} . An additional readout-type error source is imposed on the digital detector by servo-induced image motion across the digital detectors. This image motion results from servo rate following error and high frequency rate oscillation (jitter). The servo errors cause a smear of the star image on the detectors, reducing the signal-to-noise ratio and resulting in a readout of the mean image position. The gimbal encoders are modeled by quantizing the gimbal angle plus fabrication noise. One-half of an encoder bit ($EW/2$) is added (subtracted) to the gimbal encoder reading for positive (negative) gimbal rates to reduce quantization errors. After compensation, the encoder causes errors which over the long term resemble a uniformly-distributed source with a maximum value of $EW/2$ combined with a normally-distributed source of magnitude σ_{FF} caused by fabrication errors.

Gyro quantization causes a readout error. The IRU is an angle measuring device with readout con-

sisting of a series of pulses each representing an angular rotation about the input axis. The read-out error can have a maximum value of one Pulse Weight (PW) and was assumed to be uniformly distributed between 0 and 1 PW.

In addition to readout errors, the gyro outputs are in error due to gyro drift and angular noise in the gyro. Gyro drift was characterized as bias and was included in the filter state; angular gyro noise appears in the filter equations as process noise. Because a statistical description of gyro noise error did not exist, the IRU vendor was requested to perform a series of tests on an experimental version of the SPARS IRU. The data obtained from these tests were used to establish an empirical gyro noise model as described below.

Single channel gyro pulse counts (incremental angles) were accumulated over an interval of time and the total number of pulse counts recorded. This was done for one millisecond and thirty second time intervals. Analysis of the collected data indicates that each gyro channel presents data containing a one sigma error of less than one rebalance pulse. Examination of the data revealed a high correlation between millisecond samples and showed that a second harmonic of reduced magnitude is also present. The correlation function implied a harmonic component with a frequency of approximately 250 Hz. Thus the gyro noise (angle error) was modeled as a sum of a sinusoid and a white gaussian sequence.

The process noise covariance matrix Q then becomes

$$Q = C^2 \begin{bmatrix} I & O \\ O & O \end{bmatrix}$$

where I is a (3x3) Identity matrix and C is the standard deviation of gyro noise.

Small ad hoc terms also were added to each of the six diagonal elements of Q primarily to increase the elements of W relating to gyro drift bias updates.

IX. TEST RESULTS

Static and dynamic laboratory tests are described in Reference (1). Qualitative test results are described in this section and quantitative results in the classified (Secret) appendix to this report.

A. Convergence/Divergence

The SPARS attitude filter should quickly reduce large initial attitude errors, i.e., demonstrate initial convergence. Additionally, once the error in the attitude estimate converges, it should not exhibit a secular growth as more and more observations are processed by the filter. This section discusses initial convergence and long-term divergence of the

filter. Since there was a comparatively long period between receipt of the IRU and receipt of the SSA, initial convergence and long-term divergence were briefly studied by employing real IRU data and simulated SSA data.

An attitude control system was assumed which slaves the spacecraft to a local vertical/orbit plane coordinate system to within $\pm 2\text{-}1/4$ degrees.

Figure 4 shows the convergence of the attitude estimate within about five minutes in the face of initial attitude errors of $2\text{-}1/4$ degrees per axis. The first few points are off scale. The dots and asterisks denote respectively the attitude history just before and just after a filter correction.

Long-term divergence of the filter was not fully examined. There were no known significant, unmodeled, dynamical biases, a major cause of filter divergence [6]. It had been demonstrated in the SPARS Phase 0 effort that, if the gyros exhibited a drift component characterized by a random walk process, the filter would diverge if the algorithm assumed the gyro process noise was white. Static gyro test data did not reveal a random walk process. The filter was, however, designed to account for a small random walk component. The filter also employed small ad hoc terms in addition to modeling and random walk to keep the gyro drift components of the filter gain open. Figure 5 shows no apparent tendency of the filter to diverge for 6,300 seconds of operation.

B. Extended State Filter

The detailed analysis of SPARS and laboratory errors indicated the desirability of adding more state variables to the filter to reduce the effect of both system and the laboratory errors on measured attitude.

The major unmodeled errors were six SSA and star simulator alignment uncertainties. Provision was made in the test plan to estimate these biases in the SSA dynamic calibration test [1].* Theoretically these biases are observable. However, simulations showed them to be poorly observable in the comparatively short (twenty-minute) test.

Early testing of the SPARS filter employing six state variables, three representing attitude errors and three representing gyro drift biases, indicated that the unmodeled biases caused attitude errors that were slightly larger than would be predicted by the filter's estimate of the error covariance matrix. This behavior was attributed, at least in part, to the unmodeled alignment biases. Furthermore, it was felt that in orbital flight, calibration or estimation of SSA biases might be required. Therefore, a twelve-state variable SPARS filter was also designed for the laboratory testing.

An analysis showed that only ten of the twelve state variables or linear combinations of the state variable were estimable. The twelve state filter was shown by simulation and error analysis to give modest improvement in attitude over the normal twenty minute laboratory test.

Direct comparison of the six and twelve state filters was made for one test. Actual SSA, gyro and rate table data were recorded from a SPARS dynamic test employing a six state filter. The recorded sensor data was then employed to drive a simulation of the twelve state filter. The mean attitude error over the last fifteen minutes of testing showed an improvement of 33 percent. Using the twelve state filter, a 24 percent improvement in 67 percent point** was noted. Error analyses predicted a more significant improvement for longer tests.

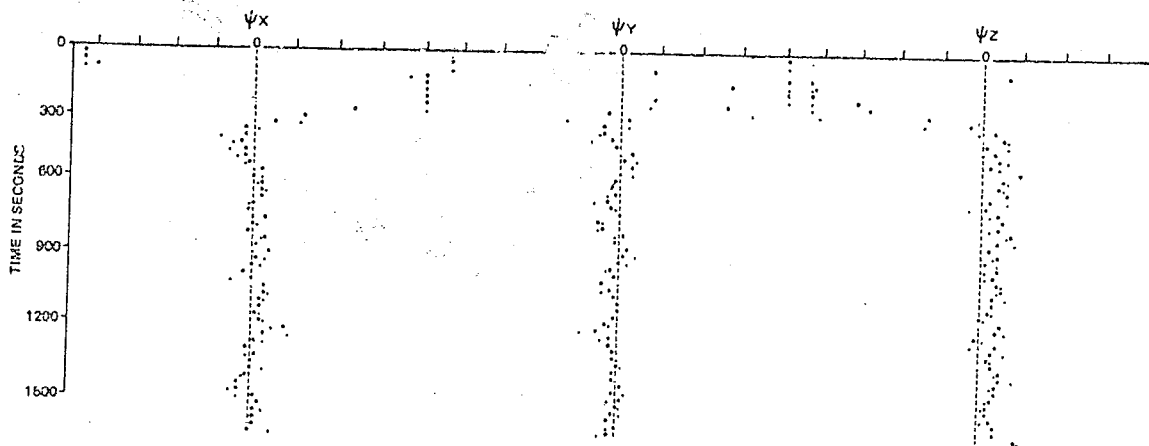


Fig. 4. Convergence from $2\text{-}1/4$ Degrees Initial Error

*A test employing only rate table and SSA data, i. e., no gyro data.

**By definition 67 percent of the measured attitude errors have magnitudes smaller than the 67 percent point.

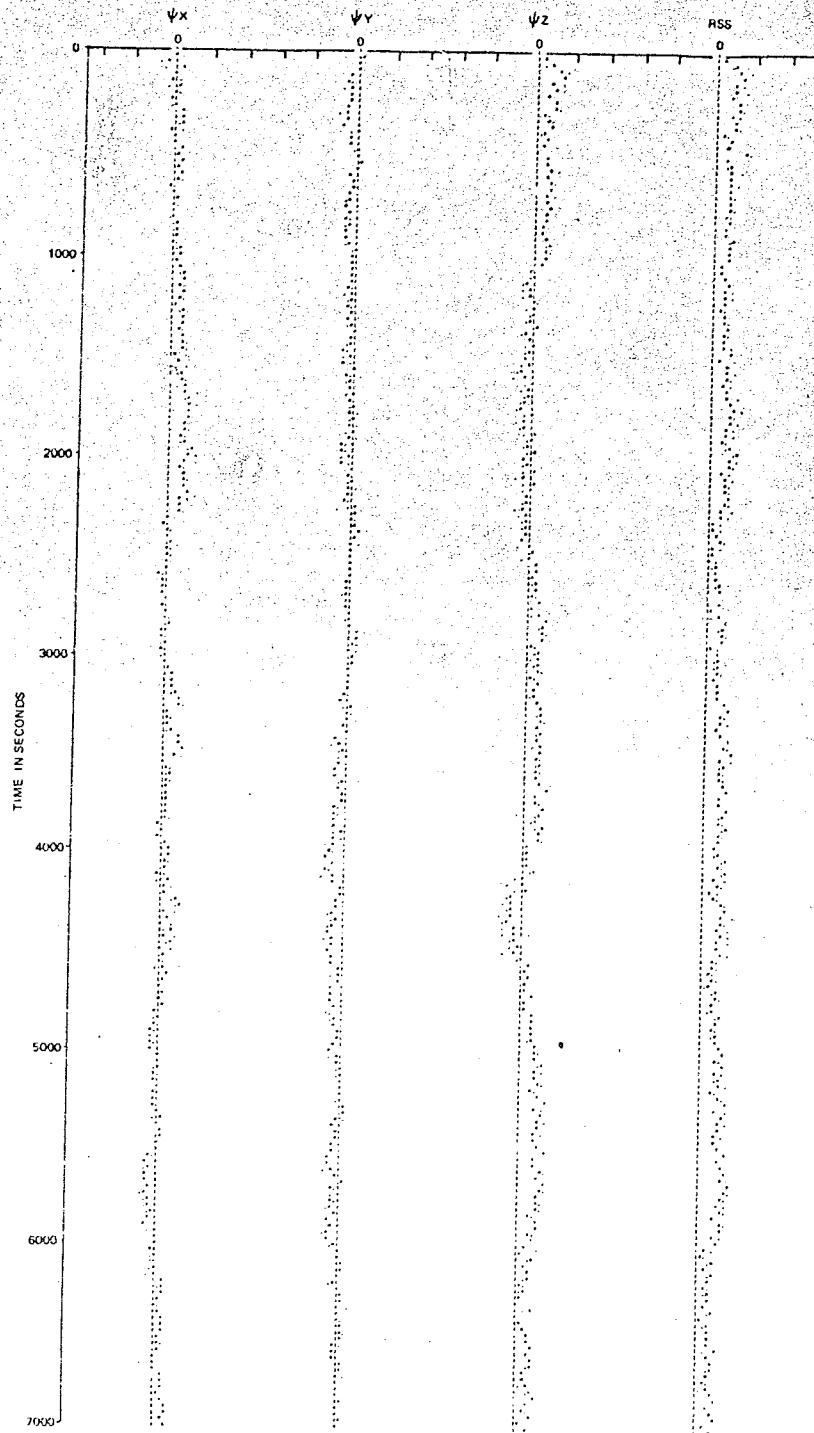


Fig. 5. Long Term Stability of Attitude Accuracy

For orbital applications, no more than 11 state variables would be employed. Due to the unobservability of two state variables the filter could be designed for nine state variables without degrading attitude accuracy.

X. CONCLUSIONS

This paper has described the configuration, algorithms and qualitative test results of a precision attitude reference system. Quantitative results are given in the classified (Secret) appendix to this paper.

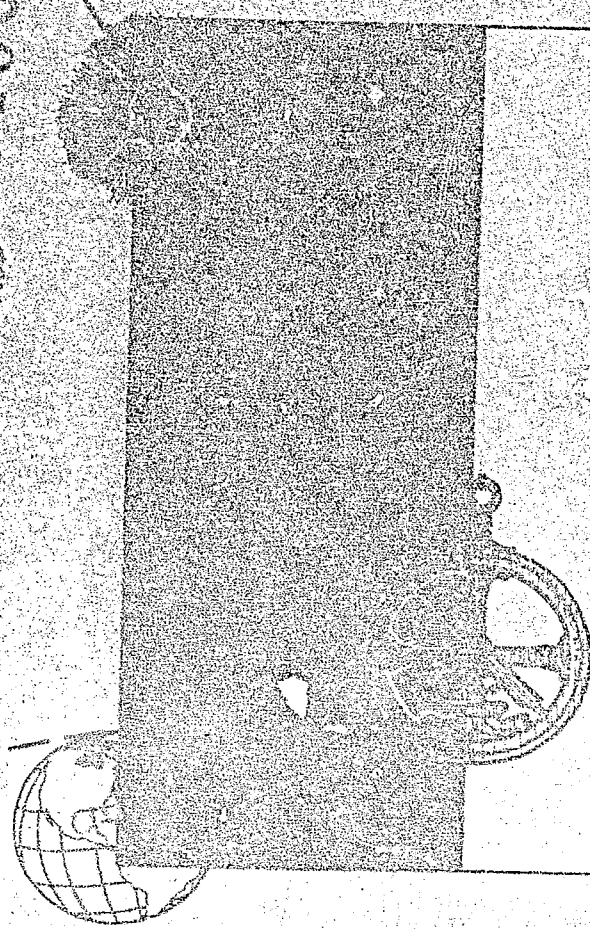
The outstanding feature of the IBM SPARS design is the use of a gimbaleed star sensor. The pointing freedom provided by a gimbaleed star sensor results in a small star catalog consisting only of the brightest and best located stars. With pointing freedom, a star is almost always available and sighting schedules can be adjusted to be as frequent as required to optimize system performance. Furthermore, the gimbaleed design can use a small telescopic FOV in order to achieve high resolution with moderate size optics.

The gimbaleed star sensor's ability to point to a star at any desired time is particularly significant during the initial acquisition phase when frequent sightings are desired to estimate attitude and drift rate parameters. Such multiple sightings could be used together with a suboptimal filter which is less sensitive to convergence difficulties than the Kalman filter. One possible technique is the deterministic filter.

REFERENCES

- [1] Schlee, F. H., Neilson, G., "Laboratory Checkout and Testing of an Advanced Stellar Inertial Attitude Reference System," Spacecraft Attitude Determination Symposium, Aerospace Corp., El Segundo, Calif., Sept. 30 to Oct. 2, 1969.
- [2] Baum, R., Sheldon, D., "A Precision Strap-down Inertial Reference Unit -- Hardware Mechanization and Test Report," Spacecraft Attitude Determination Symposium, Aerospace Corp., El Segundo Calif., Sept. 30 to Oct. 2, 1969.
- [3] Robinson, A. C., "On the Use of Quaternions in Simulation of Rigid-Body Motion," Wright Air Development Center, USAF, Wright-Patterson AFB, Ohio, Dec. 1958.
- [4] Wilcox, J. C., "A New Algorithm for Strap-down Inertial Navigation," IEEE Transactions on Aerospace and Electronic Systems, Vol AES-3, No. 5, Sept. 1967.
- [5] Bryson, A. E., and Ho, Y. C., "Applied Optimal Control," Blaisdell Publishing Company, pp. 364, 1969.
- [6] Schlee, F. H., Standish, C. J., Toda, N. F., "Divergence in the Kalman Filter," AIAA Journal, Vol. 5, No. 6, June 1967.

AD704600



*PROCEEDINGS
OF THE
SYMPOSIUM ON
SPACECRAFT
ATTITUDE
DETERMINATION*

*September 30,
October 1-2, 1969*

VOLUME I
UNCLASSIFIED PAPERS

Cosponsored by AIR FORCE SYSTEMS COMMAND
Space and Missile Systems Organization
and THE AEROSPACE CORPORATION

Held at The Aerospace Corporation
2350 El Segundo Boulevard
El Segundo, California

69 OCT 31

Reproduced by the
CLEARINGHOUSE
for Federal Scientific & Technical
Information Springfield Va 22151

D D C
DECLASSIFIED
MAR 16 1975
REVIEWED
B

THIS DOCUMENT HAS BEEN APPROVED FOR PUBLIC
RELEASE AND SALE; ITS DISTRIBUTION IS UNLIMITED

424

Air Force Report No.
SAMSO-TR-69-417, Vol I

Aerospace Report No.
TR-6066(5306)-12, Vol I

PROCEEDINGS OF THE SYMPOSIUM ON
SPACECRAFT ATTITUDE DETERMINATION,
SEPTEMBER 30, OCTOBER 1-2, 1969

Volume I: Unclassified Papers

Cosponsored by
AIR FORCE SYSTEMS COMMAND
Space and Missile Systems Organization
and THE AEROSPACE CORPORATION

Held at
THE AEROSPACE CORPORATION
2350 El Segundo Boulevard
El Segundo, California

69 OCT 31


This document has been approved for public
release and sale; its distribution is unlimited

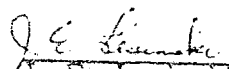
FOREWORD

These proceedings are published by The Aerospace Corporation, El Segundo, California, under Air Force Contract No. F04701-69-C-0066. Any other applicable contract number or company sponsorship is cited in a footnote on the first page of the individual paper.

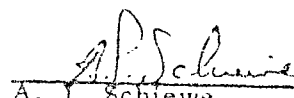
This document was submitted on 4 December 1969, for review and approval, to Captain D. Evans, SAMSO (SMTAE).


L. J. Henrikson
The Aerospace Corporation
Cochairman


D. Evans, Captain, USAF
SAMSO
Cochairman


J. E. Lesinski
The Aerospace Corporation
Cochairman

The views expressed in each paper are those of the author. Publication of this report does not constitute Air Force or Aerospace approval of the report's findings or conclusions. It is published only for the exchange and stimulation of ideas.


A. J. Schiewe
Director, Control and Sensor
Systems Subdivision
Electronics Division
Engineering Science Operations
The Aerospace Corporation


D. Evans, Captain, USAF
Project Officer

PREFACE

The Symposium on Spacecraft Attitude Determination was held at The Aerospace Corporation, El Segundo, California, on September 30 and October 1-2, 1969. It was cosponsored by the Air Force Systems Command, Space and Missile Systems Organization, and The Aerospace Corporation.

The symposium brought together 306 representatives from 44 industrial, governmental, and educational organizations concerned with spacecraft attitude determination.

The purpose of the symposium was in general to present a broad coverage of the spacecraft attitude determination problem and in particular to review the advances in sensing and data processing techniques related to spacecraft attitude determination, to assess current capabilities, and to provide an exchange of ideas among people who have an active interest in the field. The sponsors hope that the symposium has stimulated new ideas and will lead to the advancement of spacecraft attitude determination potentials.

Symposium cochairmen were D. Evans, Captain, USAF, L. J. Henrikson, and J. E. Lesinski.